

# DISTRIBUTED MATCHING SCHEME AND A FLEXIBLE DETERMINISTIC MATCHING ALGORITHM FOR ARBITRARY SYSTEMS

Yu-Chiu Chao, TRIUMF, Vancouver BC V6T 2A3, Canada

## Abstract

Paradigm complementary to conventional betatron matching is explored, with matching distributed over the entire line. This can have varying degrees of advantage over a conventional scheme.

In conjunction, a matching algorithm was developed for any line configuration, coupled 4D included, giving deterministic, rigorous optimal solutions spanning entire tradeoff curve between mismatch and quad strength, thus allowing insight and control pre-implementation. It also shows promise of attaining global optimum. Combined with distributed matching this algorithm displays further advantages of speed, determinism and flexibility.

## DISTRIBUTED MATCHING AND INTERPOLATED SOLUTION

Matching either beam ellipse or optical transport to design, in either XY coupled or uncoupled environments, has been one of the most important accelerator operation topics inspiring constant algorithmic investigation [1]. A configuration premise common to all these approaches is that the matching occurs locally, within a dedicated matching section of quadrupoles and skew quadrupoles. The current report aims to free the control paradigm from this premise and develop a supporting algorithm to enable this paradigm shift. Its implication can extend beyond matching.

### Distributed vs Local Matching Configuration

Control of accelerator and beam properties follows two distinct paradigms in terms of geometrical configuration: Distributed and Localized. These two paradigms are often characterized and justified by cost vs performance.

#### Localized Control

- Limited/Costly/Bulky hardware (monitor and actuator)
- Little chance of cumulative/compounded error
- Damage mostly confined to local areas
- Example: Dispersion, Bunch length, Energy Spread

#### Distributed Control

- More affordable and compact monitors and actuators
- Errors accumulate & compound throughout entire line
- Damage arises everywhere and is irreversible
- Example: Transverse orbit

Transverse matching shares almost all characteristics with parameters controlled in a distributed scheme, given the following features of modern accelerator systems:

- Beam profile diagnostics often form adequate coverage throughout a beam line.
- Even more dense BPM coverage has been exploited to provide AC or DC measurements of optical transport in accelerators [2].

- Quadrupoles, the actuators for matching, typically far outnumber orbit correctors.
- Beam and optical mismatch is not a local problem. It emerges and compounds at all locations and from all sources, and its adverse effects impact all sections of a beam line.

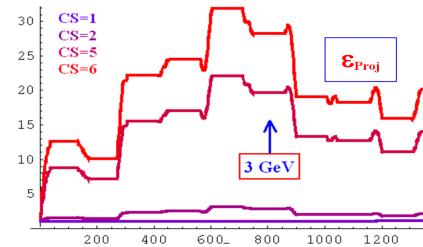


Figure 1: Projected Emittance for Various Initial Mismatch Propagated through 5 Pass CEBAF

Of the last point, cumulative mismatch not only results in excessive beam envelope and tail, it can cause more subtle damages as shown in Figure 1 [3], in which are plotted evolution paths of beam projected emittance in the Jefferson Lab CEBAF accelerator under different mismatch parameters (CS), with CS=1 for completely matched beam. Due to slight un-cancelled skew quad terms in the linac HOM couplers, the projected emittance inevitably grows. However this growth can be kept under control with a globally matched beam (CS=1). Once the projected emittance grows out of bound, no amount of quadrupole matching can bring it down. Other factors that can be exacerbated by mismatch include geometrical aberrations, nonlinear dispersive effects such as  $T_{512}$ , etc.

The reason for matching to become a localized control process, apart from specific functionality concerns, may be that historically anything less than fully matched optics out of a matching process is considered unacceptable, with no systematic procedure to evaluate its consequence or identify the follow-up action. Thus the problem is resolved by designed-in sections that must achieve 100% matching within themselves, and nowhere else. The following issues can arise with this paradigm:

- Design flexibility is limited by matching sections
- Cumulative mismatch causes problem everywhere, but is addressed only near matching sections.
- Cumulative mismatch causes excessive quad strengths.
- Excessive matching quad strengths cause local blowup.
- With all matching concentrated in localized places, there is no recourse if the solution fails.

A side product of the localized matching paradigm is often a black box optimization engine responsible for matching the beam or optics to 100%. Depending on the engine, further issues can be introduced:

- (Beam) time consuming

- Unpredictable/Inconsistent outcome
- Lack of option/insight/control on the user's part

By allowing the possibility of partial matching spread over the entire beam line, coupled to an interpolation scheme that does away with inefficiency and uncertainty, a distributed matching scheme may prove competitive where the above issues are acute, and it also leads to a rigorous and deterministic matching algorithm with physically consistent and unambiguous interpretation.

### Segmentation of Matching Sections

In a distributed matching scheme the entire beam line is segmented into sections, all contributing to the reduction of mismatch in an adiabatic manner. The segmentation is flexible and the sections need not be contiguous. Any special-purpose modules, such as RF or dispersion suppressor, can be either left out or embedded inside a matching section, as indicated in Figure 2.

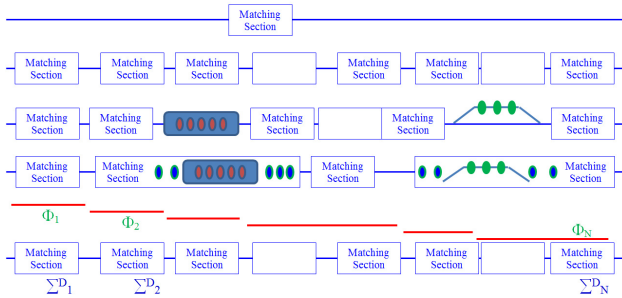


Figure 2: Concept of distributed matching. Top to bottom: (a) Localized matching (b) Segmentation into distributed matching sections, (c) Special modules left out, (d) Special modules embedded, (e) Adiabatic reduction of mismatch  $\Phi$  by partially matching to design beam covariance  $\Sigma^D$  at end of each section.

### Interpolation Scheme

The design twist  $\Sigma^D$  at end of each section in Fig. 2 is a constant. This begs the question of why matching has to be done repeatedly, and likely haphazardly, by a black box engine using beam time. Thus we look into implementing the distributed matching scheme via interpolation on pre-calculated partial matching solutions for each section. This has the following advantages:

- Speed: No online optimization needed
- Determinism: Best solution worked out a priori
- Flexibility/Controllability: User options on matching scenario such as profile of tapering mismatch  $\Phi$
- Insight into the problem can be gained given a competent offline process.

A competent algorithm will be introduced later in the note. But firstly this concept using a more naïve algorithm is demonstrated in Figure 3 for a FODO lattice with  $120^\circ$  phase advance. Each matching section contains 3 quads. With initial mismatch factor as high as 9, in 7 sections the beam is totally matched. Due to the large phase advance between quads, this process is not overly demanding numerically.

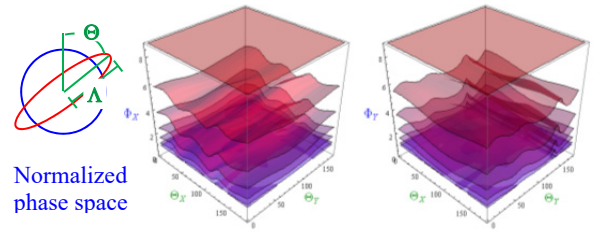


Figure 3: Applying distributed matching to a  $120^\circ$  lattice. Initial mismatch of  $\Phi=9$  in both X & Y is launched into the line, with mismatch angle  $\Theta$  covering entire range of 0 to  $\pi$ . The color sheets represent the evolution of  $\Phi_{X/Y}$  at all initial  $\Theta_{X/Y}$  through 7 distributed matching sections. Solution at each section is interpolated from offline table.

## RIGOROUS DETERMINISTIC MATCHING ALGORITHM

### Trade-off Between Objective and Constraint

By allowing the possibility of partial matching solutions we have the opportunity of rigorously examine the interplay between matching objective and other factors limiting it. The canonical approach for studying this interplay is that due to Lagrange

$$\begin{cases} \nabla F = \lambda \cdot \nabla H \rightarrow k_1^0, k_2^0, k_3^0, \dots, k_N^0, \lambda^0 \rightarrow F = f(h) \\ H = h \end{cases}$$

where an objective function  $F$  of  $k_m$  to be optimized is subject to constraint function  $H$  of the same  $k_m$ . The solution is obtained by imposing the tangency condition with an arbitrary variable  $\lambda$ , and specifying the particular value of  $H=h$ . This amounts to asking what the optimal value is for  $F$  as a function of  $h$ . By scanning over  $h$  we get a complete picture of the objective  $F$  played against the constraint  $H$  in a locally optimal sense everywhere. Equivalently, one can scan  $f$ , or even  $\lambda$ , to get an alternative view of the same trade-off [4].

$$\begin{cases} \nabla F = \lambda \cdot \nabla H \rightarrow k_1^0, k_2^0, k_3^0, \dots, k_N^0, \lambda^0 \rightarrow H = h(f) \\ F = f \end{cases}$$

$$\nabla F = \lambda \cdot \nabla H \rightarrow k_1^0, k_2^0, k_3^0, \dots, k_N^0 \rightarrow \begin{cases} F = f(\lambda) \\ H = h(\lambda) \end{cases}$$

The three formulations above for mapping out trade-off between objective and constraint can be shown to lead to differential relations between the optimal solution  $\mathbf{k} = (k_1^0, k_2^0 \dots k_N^0)$  and  $f, h$  or  $\lambda$ :

$$\begin{aligned} \left. \frac{d\mathbf{k}}{df} \right| &= \frac{1}{\lambda} \cdot \frac{\mathbf{M}^{-1} \cdot \mathbf{R}}{\mathbf{R}^T \cdot \mathbf{M}^{-1} \cdot \mathbf{R}} = \frac{1}{\lambda} \cdot \frac{\text{Adj}(\mathbf{M}) \cdot \mathbf{R}}{\mathbf{R}^T \cdot \text{Adj}(\mathbf{M}) \cdot \mathbf{R}} \\ \left. \frac{d\mathbf{k}}{dh} \right| &= \frac{\mathbf{M}^{-1} \cdot \mathbf{R}}{\mathbf{R}^T \cdot \mathbf{M}^{-1} \cdot \mathbf{R}} = \frac{\text{Adj}(\mathbf{M}) \cdot \mathbf{R}}{\mathbf{R}^T \cdot \text{Adj}(\mathbf{M}) \cdot \mathbf{R}} \\ \left. \frac{d\mathbf{k}}{d\lambda} \right| &= \mathbf{M}^{-1} \cdot \mathbf{R}, \quad \mathbf{k} = (k_1^0(\lambda), k_2^0(\lambda), \dots, k_N^0(\lambda)) \\ \mathbf{M}_{ij} &= \frac{\partial^2 (F(\mathbf{k}) - \lambda \cdot H(\mathbf{k}))}{\partial k_i \partial k_j}, \quad \mathbf{R}_i = \frac{\partial H(\mathbf{k})}{\partial k_i} \\ \text{Adj}(\mathbf{M}) &= \text{Cof}(\mathbf{M})^T = \text{Det}(\mathbf{M}) \cdot \mathbf{M}^{-1} \end{aligned}$$

where the vertical bar limits the derivative to be taken only along the 1-dimensional curve of optimal tradeoff. The above formulas in principle make possible a

deterministic program of integration from optimal constraint to optimal objective and vice versa, including all optimal tradeoff solutions in between. Of the 3 differential relations, the one w.r.t.  $\lambda$  is most crucial:

- This formulation has universal starting ( $-\infty$ ) and ending (0) values for  $\lambda$ , independent of problem detail, thus giving unequivocal start and end points of the process.
- Integration over  $f$  and  $h$  alone will encounter singularities ( $R^T \cdot Adj(M) \cdot R = 0$ ) that can be resolved only by complementary process over  $\lambda$  at these points.

**Betatron Matching Algorithm**

For the most generic 4D betatron matching problem under constraint of minimal RMS deviation of  $N_Q$  quadrupole strengths from design, we take

$$F = \frac{1}{4} Tr \left( \Sigma_D^{-1} \cdot M(k_m) \cdot \Sigma_R \cdot M^T(k_m) \right)$$

$$m = 1, 2, \dots, N_Q$$

$$\Sigma^{ij} = \frac{1}{n} \sum_{k=1}^n x_k^i \cdot x_k^j \quad i, j = 1, 2, 3, 4$$

$$H = \sum_{m=1}^{N_Q} (k_m^R - k_m^D)^2 = \sum_{k=1}^{N_Q} \delta k_m^2$$

where  $\Sigma_D$  and  $\Sigma_R$  are the design and real beam covariance and  $M$  the transfer matrix of the  $N_Q$  quad section.  $F$  can be regarded as a 4D extension of the 2D mismatch factor. The generic formulation allows using other performance objectives and constraints, although the example above is very well behaved even for very difficult optics. Figure 4 shows a representative case where the entire tradeoff is mapped out for a 6 quad, 30° per cell FODO lattice. This is a much more difficult problem numerically than the 120° case numerically due to low phase advance. Robustness and ability to reach the final optimum of the algorithm are explained in the caption. The true power of this algorithm is revealed in Figure 5 showing the same solution plotted in the  $h-f$  plane. While a typical local optimization algorithm might have stopped at  $f=1.00013$  (C2 of Fig. 4) and declared success, it is clear from the current algorithm that the optimization as not stopped until  $\lambda=0$ , and we are rewarded with a much lower RMS quad strength. This characteristic property of the algorithm allows us to extract a simple subset of the complex solution path that corresponds to the “global” optimum for both objective and constraint, as shown in Fig. 5.

Additional tests of the algorithm, including restoring transport error causing mismatch factor up to several 1000 further demonstrate its robustness, self-consistency, and very low demand for human intervention in terms of fine tuning run parameters, an important feature if this algorithm is to be used for generating massive interpolation tables. We are also looking into expanding the repertoire of objectives and constraints, to functions such as weighted mismatch factor, weighted or absolute quad RMS, phase advance, matrix elements, etc. Even if the optima for these functions are not known a priori, the algorithm introduced here can take advantage of the

known trivial optimum for  $H$ , at  $\delta k_m = 0$ , to integrate to the optima at either the new objective or constraint [4].

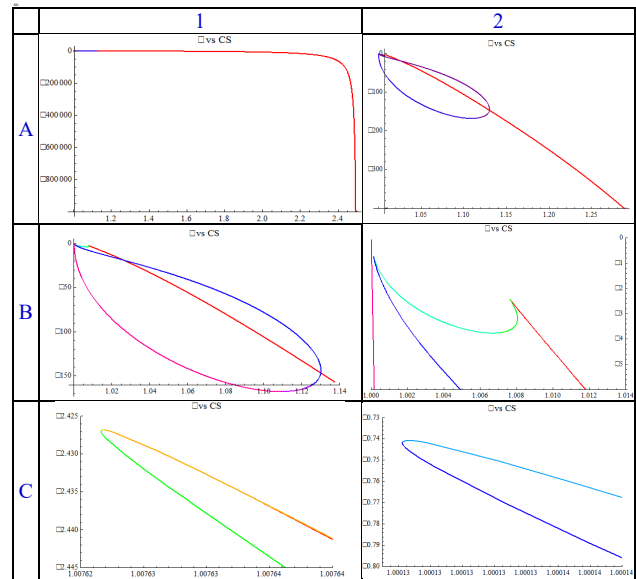


Figure 4: Entire solution path in the  $\lambda$ - $f$  plane for a 6-quad 30° per cell FODO lattice, zoomed at different locations. **A1**: Global solution path starting at ( $f=2.5, \lambda \rightarrow -\infty$ ), ending at ( $f=1, \lambda=0$ ). **A2**: Zoomed in for detail toward the end. **B1**: Further zoom. **B2**: Near the point  $\lambda=0$  and  $f=1$ : The path first approaches absolute optimum near  $f=1.0076$ , then at  $f=1.00013$  (!), then executing a loop all the way down to  $f=1.14$  before turning around and reaching the true  $f=1$  point, shown by the red line on the extreme left.. **C1**: Zoom in around  $f=1.0076$ , the turn-around on the right in B2. **C2**: Zoom in around  $f=1.00013$ , the turn-around on the left in B2.

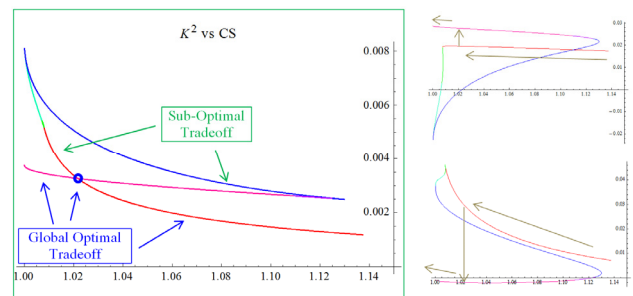


Figure 5: Left: Solution path in the  $h$ - $f$  plane roughly corresponding to B1 in Figure 4. By insisting on not stopping at  $f=1.00013$  and press on to  $\lambda=0$ , we reached the true ‘global’ optimum with a much lower RMS quad strength. This illustrates how a globally optimal tradeoff curve can be extracted by joining the red section with the magenta section at the intersection (blue circle), and discard everything above and to the right. Right: Examples showing two quadrupole  $k$  vs  $f$  plots with the path of globally optimal tradeoff indicated by gold arrows. Start with the red curve, then jump to the magenta curve at  $f(\text{CS})=1.02$ , the blue circle location on the left plot. The fact that  $\lambda$  is negative everywhere makes this process unambiguous for both  $f$  and  $h$ .

Copyright © 2015 CC-BY-3.0 and by the respective authors

**REFERENCES**

- [1] See for example Y. Chao, “A Full-Order, Almost-Deterministic Optical Matching Algorithm”, Proceedings of the 2001 Particle Accelerator Conference.
- [2] V. Lebedev et al., “Linear Optics Correction in the CEBAF Accelerator,” Proceedings of the 1997 Particle Accelerator Conference.  
Y. Chao, “Measuring and Matching Transport Optics at Jefferson Lab,” Proceedings of the 2003 Particle Accelerator Conference.
- R. Bodenstein et al., “Real Beam Line Optics from a Synthetic Beam”, Proceedings of the 2010 International Particle Accelerator Conference.
- [3] Y. Chao, “Generation and Control of High Precision Beams at Lepton Accelerators”, Proceedings of the 2007 Particle Accelerator Conference.
- [4] Y. Chao, “A Deterministic Program for Obtaining Optima under Constraints for Any Analytical System“, ARXIV:1508.01846V2 [MATH.OC]